

Remodeling of mechanical junctions and of microtubule-associated proteins accompany cardiac connexin43 lateralization

Halina S. Chkourko, MS,^{*†} Guadalupe Guerrero-Serna, PhD,[‡] Xianming Lin, PhD,^{*} Nedal Darwish, BS,^{*} Joshua R. Pohlmann, BS,[§] Keith E. Cook, PhD,^{||} Jeffrey R. Martens, PhD,[¶] Eli Rothenberg, PhD,[#] Hassan Musa, PhD,[‡] Mario Delmar, MD, PhD, FHRS^{*}

From ^{*}The Leon H. Charney Division of Cardiology, New York University School of Medicine, New York, New York, Departments of [†]Molecular and Integrative Physiology, [‡]Medicine (Division of Cardiovascular Medicine), [§]Surgery, ^{||}Biomedical Engineering, and [¶]Pharmacology, University of Michigan Medical School, Ann Arbor, Michigan, and [#]Department of Biochemistry, New York University School of Medicine, New York, New York.

BACKGROUND Desmosomes and adherens junctions provide mechanical continuity between cardiac cells, whereas gap junctions allow for cell-cell electrical/metabolic coupling. These structures reside at the cardiac intercalated disc (ID). Also at the ID is the voltage-gated sodium channel (VGSC) complex. Functional interactions between desmosomes, gap junctions, and VGSC have been demonstrated. Separate studies show, under various conditions, reduced presence of gap junctions at the ID and redistribution of connexin43 (Cx43) to plaques oriented parallel to fiber direction (gap junction “lateralization”).

OBJECTIVE To determine the mechanisms of Cx43 lateralization, and the fate of desmosomal and sodium channel molecules in the setting of Cx43 remodeling.

METHODS Adult sheep were subjected to right ventricular pressure overload (pulmonary hypertension). Tissue was analyzed by quantitative confocal microscopy and by transmission electron microscopy. Ionic currents were measured using conventional patch clamp.

RESULT Quantitative confocal microscopy demonstrated lateralization of immunoreactive junctional molecules. Desmosomes and gap junctions in lateral membranes were demonstrable by electron microscopy. Cx43/desmosomal remodeling was accompanied by

lateralization of 2 microtubule-associated proteins relevant for Cx43 trafficking: EB1 and kinesin protein Kif5b. In contrast, molecules of the VGSC failed to reorganize in plaques discernable by confocal microscopy. Patch-clamp studies demonstrated change in amplitude and kinetics of sodium current and a small reduction in electrical coupling between cells.

CONCLUSIONS Cx43 lateralization is part of a complex remodeling that includes mechanical and gap junctions but may exclude components of the VGSC. We speculate that lateralization results from redirectionality of microtubule-mediated forward trafficking. Remodeling of junctional complexes may preserve electrical synchrony under conditions that disrupt ID integrity.

KEYWORDS Connexin; Desmosomes; Sodium current; Gap junctions; EB1; Kinesin

ABBREVIATIONS Cx43 = connexin43; ID = intercalated disc; I_{Na} = sodium current; LM = lateral membrane; OS = Online Supplement; PG = protein plakoglobin; PH = pulmonary hypertension; PKP2 = plakophilin-2; RV = right ventricle/ventricular; VGSC = voltage-gated sodium channel

(Heart Rhythm 2012;9:1133–1140) © 2012 Heart Rhythm Society. All rights reserved.

Introduction

Intercellular communication is essential for cardiac function. Mechanical continuity is provided by desmosomes and adherens junctions, whereas gap junctions provide a low-resistive pathway between cells. These complexes preferentially reside at the intercalated disc (ID). Also resident to the

ID are “nonjunctional” molecules, that is, not involved in providing a physical continuum between cells. Conventionally, the various ID molecules, junctional or not, have been considered separate entities. Yet, this view is rapidly changing and the emerging picture is that of the ID as a protein interacting network involved in maintaining synchrony within cell populations.^{1–3}

The importance of gap junctions in normal electrical function is well established. Recent studies have shown that under various pathological conditions, there is reduced presence of gap junction plaques at the ID, often replaced by neoformation of gap junctions at sites other than the cells’ edge (see, eg, references^{4–9}). Changes in the total abundance of connexin43 (Cx43) have also been reported (eg,

This study was supported by National Institutes of Health (grant numbers HL106632, HL087226, and GM57691 to Dr Delmar and T32-HL007853 to Dr Guerrero-Serna) and a Foundation Leducq Transatlantic Network (to Dr Delmar). **Address for reprint requests and correspondence:** Dr Mario Delmar, MD, PhD, The Leon H. Charney Division of Cardiology, New York University School of Medicine, 522 First Avenue, Smilow 805, New York, NY 10016. E-mail address: Mario.Delmar@nyumc.org.

reference 5). This process of gap junction “remodeling” has been described as a potential substrate for cardiac arrhythmias.^{6,10} Yet, it can be argued that if the lateral membrane junctions are functional, lateralization may help to maintain action potential propagation. Either as an arrhythmogenic event or as an antiarrhythmic event, gap junction remodeling is a process intrinsic to cardiac pathology and, likely, highly relevant to the heart rhythm.

The formation of Cx43-mediated gap junctions requires preformation of mechanical junctions.¹¹ Thus, we speculate that to be functional, the redistribution of Cx43 should be accompanied by remodeling of mechanical junctions. Moreover, the mechanisms that transport Cx43 to its new location remain unclear. We propose that Cx43 lateralization involves redirectionality of microtubule-mediated Cx43 trafficking^{12,13} to the lateral membrane. Furthermore, while intercellular junctions associate with the voltage-gated sodium channel (VGSC) complex at the ID,^{14–16} the fate of that interaction once remodeling has been triggered remains undefined. Here, we have characterized junctional remodeling in an ovine model of right ventricular pressure overload.^{17–25} The data show substantial Cx43 lateralization. Cx43 plaques oriented parallel to fiber direction colocalized with mechanical junction proteins and with the microtubule-associated proteins EB1²⁶ and Kif5b.^{27–29} Separate electron microscopy studies demonstrated the presence of desmosomes and gap junctions at sites of side-side contact. In contrast, our data suggest that VGSC remodeling may follow a process different from that of junctional proteins, with consequent functional changes in the amplitude and kinetics of sodium current (I_{Na}). Overall, this is the first characterization of the fate of the desmosome-gap junction-VGSC complex under pressure-overload–induced remodeling. These observations provide a fundamental background to understand intercellular communication in cardiac disease, particularly in cases affecting mechanical continuity between cells.

Methods

Pulmonary hypertension (PH) was induced in adult sheep by injection of sephadex beads in the right ventricular (RV) chamber, as previously described (see references^{19–21} and Online Supplement [OS]). Ketorolac (60 mg intravenous) was administered prior to the injection of beads. Anesthesia was induced with 60–90 mg/kg of propofol and maintained after endotracheal intubation with 1%–3% inhaled isoflurane. Animals were monitored during anesthesia by continuous tracking of arterial heart rate and blood pressure and intermittent examination of jaw tone. Euthanasia was carried out by intravenous injection of Fatal-Plus (pentobarbital sodium at 86.2 mg/kg). All animal use was consistent with guidelines from the National Institutes of Health and approved by institutional committees.

Colocalization of Cx43 with desmosomal proteins (protein plakoglobin [PG], desmocollin, desmoglein, desmoplakin [DP], plakophilin-2 [PKP2]), N-cadherin, ankyrin G, Nav1.5, EB1, and Kif5b was assessed by immunohisto-

chemistry of RV tissue of control sheep and of sheep afflicted with PH. Confocal microscopic images were utilized for the quantitative analysis of the directionality of immunoreactive plaques and the colocalization of fluorescent signals. Electron microscopy was used to identify junctional complexes at the sites of side-side apposition between cells, whereas total internal reflection fluorescence was used to demonstrate colocalization of Kif5b and Cx43 in freshly isolated mouse cardiomyocytes. Sodium and gap junction currents were characterized in cardiomyocytes isolated from right and left control and PH sheep ventricular tissue. Methods are described in detail in the OS.

Results

Cx43 remodeling in the RV of sheep subjected to RV pressure overload

In control animals, Cx43 signal in the RV oriented primarily perpendicular to fiber orientation (corresponding to ID; Figure 1A). In contrast, long clusters of immunoreactive signal oriented parallel to the fibers were found in the RV of sheep subjected to RV pressure overload (Figure 1B). From a total of 84 plaques analyzed in control tissue, 60 were deemed perpendicular (71% of the total), only 8 were found to be parallel to the orientation of the fibers, and 16 were classified as “undefined” (Figure 1C; see OS for details on the methods of analysis). In contrast, of the 403 plaques analyzed in the RV tissue of PH animals, only 34% were perpendicularly oriented (Figure 1D). These results indicate that in this model, Cx43 undergoes extensive remodeling, with increased predominance of plaques oriented parallel to the fibers’ axis. For simplicity, plaques oriented in the perpendicular or parallel direction will be referred to as “ID” (for “intercalated disc”) or “LM” (for lateral membrane), respectively. Regions of interest with an ambiguous orientation were not included in colocalization analysis.

Proteins of mechanical junctions accompany Cx43 remodeling

Immunostaining of the desmosomal/adherens junction PG showed a pattern similar to that observed for Cx43, with plaques localized to the ID in control (Figure 1E) and redistributed in parallel direction in PH hearts (Figure 1F). From a total of 79 PG plaques analyzed in control tissue, 59 were identified as perpendicular (75%), 13 (16%) were undefined, and 7 (9%) were parallel (OS Figure 1A). In PH hearts, only 42% of the plaques (out of 437 total) were perpendicular (ie, at the ID; see OS Figure 1B). Overlay of signals showed cosegregation of Cx43 and PG to the same cellular region (Figures 1G and 1H). An enlarged image of the plaque formed at the lateral membrane displays the characteristic pattern of colocalization of desmosomal and gap junction proteins,³⁰ with either overlapping or alternating pixels positive for one protein or another (Figure 1; panels a, a’, and a’'). A Pearson’s coefficient analysis showed that compared with control, the probability of ID colocalization was significantly decreased in PH hearts (Figure 1I). Pearson’s coefficient for signals oriented paral-

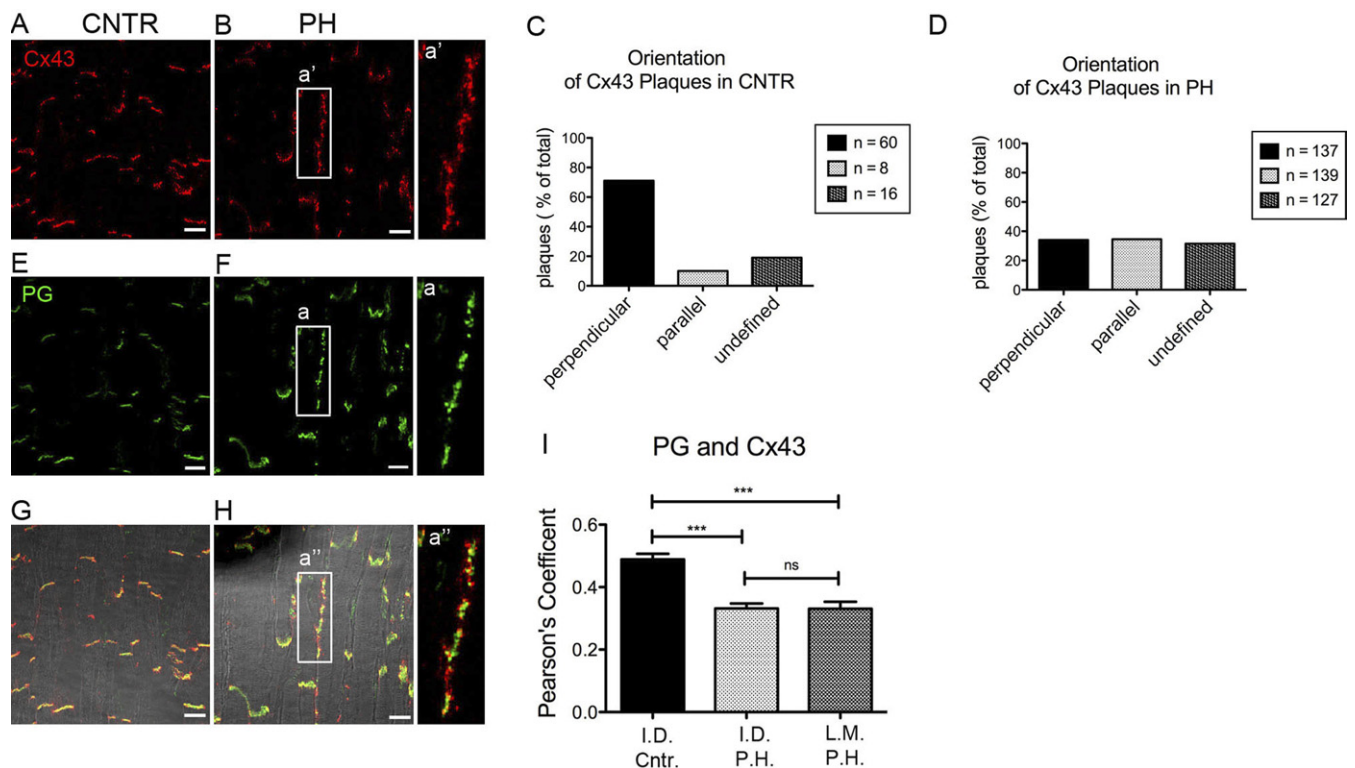


Figure 1 Localization of connexin43 (Cx43) and plakoglobin (PG). Confocal microscopy images from right ventricular tissue of control sheep (CNTR) (A, E, G) or sheep with pulmonary hypertension (PH) (B, F, H). Immunoreactive Cx43 (red) and PG (green) are presented separately (A, B), and (E, F) in merged images (G, H). a, a', a' enlarged images of Cx43 and PG along the long axis. Bar = 20 μ m. C and D: Quantification plots representing percentage of Cx43 plaques found in a given orientation with respect to fiber direction in tissue CNTR (C) or PH (D). Total number of plaques: 84 (CNTR) and 403 (PH). I: Colocalization (Pearson's coefficient) of PG and Cx43 in plaques oriented perpendicular (intercalated disc [ID]) or parallel (lateral membrane [LM]) to fiber orientation. Statistical analysis: 1-way analysis of variance, Tukey's multiple comparison test. Mean \pm SEM. P : >.05 (ns); .001–.0001 (***). Numbers of regions of interest analyzed: 48, 60, and 60 for ID CNTR, ID PH, and LM PH, respectively. SEM, standard error of the mean.

lel to fibers (LM) was not carried out in control preparations, given the very low number of regions of interest oriented in that direction (see also Figure 1C). Yet, in PH hearts, we observed a degree of colocalization similar to that found in the ID, suggesting that the displacement of Cx43 to LMs is accompanied by the redistribution of mechanical junction proteins. To further extend this concept, we examined the localization of the desmosomal cadherins desmocollin (OS Figures 1C and 1D; OS Figure 2) and desmoglein (OS Figures 1E and 1F; OS Figure 3), the desmosomal components PKP2 (OS Figures 1G and 1H; OS Figures 4A and 4B), and desmoplakin (OS Figures 1I and 1J; OS Figures 4C and 4D) as well as N-cadherin (a component of the area composita^{31,32}; OS Figures 1K and 1L; OS Figures 4E and 4F). Consistently, we observed a decrease in the fraction of plaques at the ID, and an increase in those parallel to the fibers, in PH hearts. We also observed a decrease in the extent of colocalization (Pearson coefficient) of Cx43 with other junctional proteins at the ID, except for desmocollin and N-cadherin, in PH hearts when compared with control. Pearson coefficient values at the LM were significantly lower than at the ID (except in the case of PG); yet, for all proteins of the area composita tested, the probability of colocalization with Cx43 at the LM was higher than 20% and significantly larger than zero. These data

suggested that the lateralization of Cx43 was not an isolated event but part of a complex remodeling process that includes molecules necessary for mechanical junction formation. Western blot analysis was limited by the availability of antibodies immunoreactive to ovine tissue. Changes in protein abundance were not detected (see OS Figure 5).

Desmosomes and gap junctions in the LM of cardiac tissue

The data in Figure 1 and Online Supplemental Figures 1–4 suggest that desmosomal and gap junction molecules are able to form new complexes even if displaced from the ID. More direct demonstration was obtained by electron microscopy (Figure 2). The low-resolution image in Figure 2A reveals the preserved morphology of a thin section from the RV of a PH-afflicted heart. Fiber orientation can be distinguished. An enlargement of the area demarcated by the red box, corresponding to a site where cardiac cells are in close lateral (not end-end) proximity, is presented in Figure 2B. The image shows 2 types of electron-dense structures interrupting the continuity of the intercellular space: one with the morphological characteristics of a desmosome, and the other with the morphological features of a gap junction plaque. These results provide

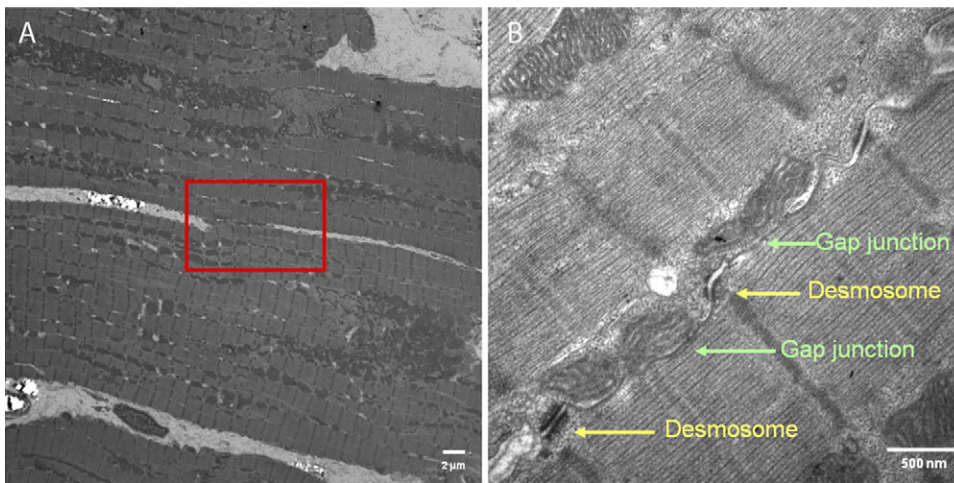


Figure 2 Electron microscopy image obtained from the right ventricle of a sheep afflicted with pulmonary hypertension. Low-magnification image = 2600 \times (A), shows preservation of structures and orientation of cells. Area within the red square is shown in B, at higher magnification = 34,000 \times . Notice the presence of lateralized desmosomes and gap junctions oriented parallel to fiber direction.

evidence that junctional structures can be formed at the LMs of cardiac myocytes. The formation of these structures likely facilitates the preservation of electrical coupling even when the molecular organization of the ID is disturbed.

Junctional remodeling and the fate of the VGSC complex

Previous studies show that the sodium channel protein $Na_V1.5$ localizes primarily to the ID and associates with junctional molecules.^{1,14–16} We therefore explored whether

the VGSC complex is also redistributed to the LM. $Na_V1.5$ -immunoreactive plaques at the ID were clearly visible in control tissue, colocalizing with Cx43 (Figure 3A; labeled CNTR; $Na_V1.5$ in red, Cx43 in green; overlay in bottom panels; box labeled “a” enlarged in right panels). In contrast, the $Na_V1.5$ plaques were very sporadic in PH hearts. Most of the lateralized Cx43 signals were void of a colocalizing $Na_V1.5$ signal (see boxes labeled “b”) though occasional overlap was seen at the ID (“c”). As a result, the Pearson coefficient for the colocalization of Cx43 and $Na_V1.5$ was significantly decreased, particularly in the LM

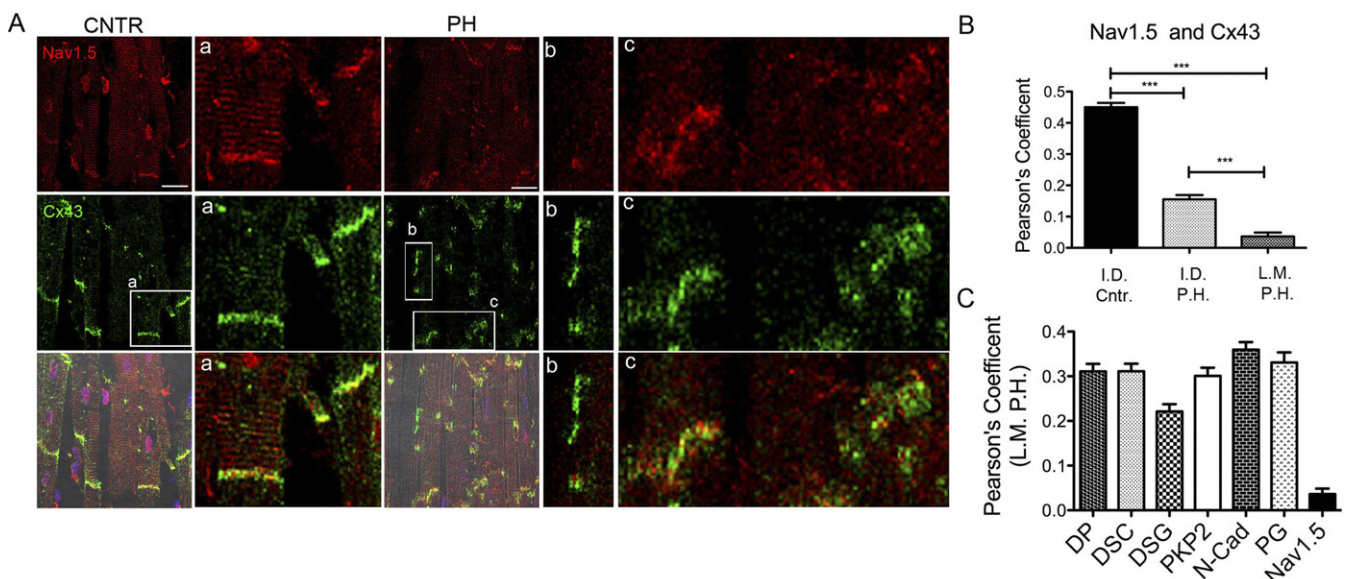


Figure 3 $Nav1.5$ localization in PH hearts. **A:** Confocal microscopy images obtained from CNTR or PH sheep. $Nav1.5$ (red), Cx43 (green). **a:** Enlarged area of intercalated disc (ID) from CNTR animal. Notice colocalization of $Nav1.5$ and Cx43 highlighted by yellow in merged image. **b:** Enlarged area of Cx43 with $Nav1.5$ along the long axis in PH tissue. Notice absence of immunoreactive $Nav1.5$ where immunoreactive Cx43 is present. **c:** Enlarged images of Cx43 and $Nav1.5$ of 2 IDs. Notice presence of immunoreactive $Nav1.5$ (red) in “left” ID and its loss in “right” one. Scale bar = 20 μm . **B:** Quantification of colocalization (Pearson's coefficient) of $Nav1.5$ and Cx43 signals at areas of ID in CNTR and PH animals and at the lateral membrane (LM) of PH animals. Statistical analysis: 1-way analysis of variance, Tukey's multiple comparison test. Mean \pm SEM. P : .001–.0001 (***). Numbers of regions of interest analyzed: N = 61, 108, and 50 for ID CNTR, ID PH, and LM PH, respectively. **C:** Comparison of Pearson coefficient values for colocalization of Cx43 with various molecules (noted in abscissae) at LM in PH hearts. Analysis of variance-Tukey's multiple comparison test showed that the value obtained for Cx43- $Nav1.5$ colocalization was highly different from that obtained for all other junctional molecules ($P < .0001$). CNTR = control; DP = desmoplakin; DSC = desmocollin; DSG = desmoglein; Cx43 = connexin43; N-Cad = cadherin; PG = plakoglobin; PH = pulmonary hypertension; PKP2 = plakophilin-2; SEM, standard error of the mean.

region (Figure 3B), where this value was not different from zero (2-tailed *t* test). Furthermore, the analysis of variance-Bonferroni test for all LM Pearson coefficient values showed that the extent of colocalization of Cx43 with Nav1.5 was significantly less than that obtained for junctional molecules (Figure 3C). These data suggest that while junctional molecules reorganize to form junctional complexes “in exile,” Nav1.5 molecules do not follow. Ankyrin G detection was hampered by high background and as such, quantitative analysis for colocalization at the LM was not possible; yet, immunofluorescence images suggest that in PH hearts, ankyrin G localization at the ID decreased significantly (see OS Figures 1M and 1N; OS Figure 6). As a next step, we asked whether the reported changes in protein localization were associated with modifications in I_{Na} properties.

ID remodeling and electrophysiological properties

Electrophysiological recordings were obtained from cardiac myocytes isolated from the left ventricle or the RV of afflicted animals, as well as from the RV of control animals. As shown in Figure 4A, average current density recorded from left ventricle cells was slightly larger than from cells dissociated from control RV. This difference became more noticeable when cells from the RV of afflicted animals were tested (Table 1). The decrease in peak current density was accompanied by a slight shift in peak current voltage relation (Figure 4A), a significant decrease in $V_{1/2}$ activation (Figure 4B; Table 1), and a slowing in recovery from inactivation (Figure 4D) without a noticeable change in voltage dependence of steady-state inactivation (Figure 4C). Overall, these results indicate that pressure overload led to changes not only in distribution but also in function of the VGSC complex. Similarly, as shown in Figure 4E, we observed an $\sim 30\%$ decrease in junctional conductance measured between myocytes from an afflicted RV when compared with control. Of note, ventricular arrhythmias, or unexplained sudden death, have not been observed in these animals and are not clinical features of patients with PH.^{20,23}

Lateralized Cx43 and redistribution of molecules involved in Cx43 forward trafficking

The mechanism by which Cx43 reaches the LM of the cell remains poorly understood. We speculate that Cx43 lateralization results, at least in part, from rerouting of Cx43 forward trafficking to a new microdomain. A key molecule in Cx43 forward trafficking is the microtubule-associated end-plus protein EB1, which tethers to N-cadherin for the delivery of Cx43.²⁶ In Figure 5 we show that under control conditions, EB1 (green) colocalized with Cx43 (red) at the ID (box and panels labeled “a”). In PH hearts, EB1–Cx43 colocalization was maintained, but in this case, plaques oriented parallel to the cells (box and panels labeled “b”). Overlay images (bottom of Figure 5) showed that regardless of the position of the plaque, there was overlap or close alternation of immunofluorescent signals, indicating close

proximity of the 2 proteins. These results suggest that pressure overload led to lateralization of EB1. Separately, we showed that kinesin protein Kif5b, a microtubule-associated motor protein in the heart, also colocalized with Cx43, both in control and in PH hearts (Figure 6A). To confirm this observation and minimize the influence of background fluorescence, we utilized total internal reflectance fluorescence microscopy in isolated adult mouse cardiac myocytes. As shown in Figure 6B, there was abundant colocalization of Cx43 and Kif5b at the end of the cell, consistent with the hypothesis that this kinesin participates in microtubule-dependent trafficking of ID proteins, including Cx43.

Discussion

Mechanical junctions are an integral component of cardiac mechanical and electrical function. Yet, the fate of mechanical junction proteins in the setting of heart disease remains understudied. Here, we utilized an animal model of RV pressure overload to characterize the morphology of intercellular junctions formed outside the area of the ID. We show gap junction neoformation concurrent with remodeling of mechanical junction proteins. Yet, these new complexes showed limited association with Nav1.5 and functionally, a reduction in amplitude and change in kinetics of the I_{Na} . While Cx43 remodeling has been previously described, this is the first characterization of the fate of the desmosome-gap junction-VGSC complex in a model of cardiac pressure overload. It is important to emphasize that we did not implement this model to study cardiac arrhythmias. Rather, we did this as a system to characterize, in a living animal, the fate of various ID proteins. In fact, we speculate that in this case, the redistribution of junctional proteins allows for—partial—preservation of electrical communication. Electrophysiological recordings showed only a minor decrease in junctional conductance (see Figure 4). It is worth noting that no Cx43 lateralization (only loss of Cx43 plaques) has been reported in hearts of patients with arrhythmogenic right ventricular cardiomyopathy, an inherited disease associated with mutations in desmosomal proteins. It is interesting to note that in our case, N-cadherin was also prominent at the LM, in contrast to what has been observed in cases of arrhythmogenic right ventricular cardiomyopathy.

We have previously shown that loss of expression of the desmosomal protein PKP2,¹ as well as loss of Cx43 expression,² affects I_{Na} function. In the PH heart, gap junctions and desmosomes formed at a new site, but Nav1.5 did not reorganize in a similar manner. We speculate that as opposed to gap junctions and desmosomes, trafficking of Nav1.5 requires molecules that are unable to redirect to the LMs. Furthermore, our data showed significant slowing of recovery from inactivation for I_{Na} . Interestingly, similar effects were recently reported for Nav1.5 channels exposed to membrane stretch.³³ It is tempting to speculate that kinetics can be changed by moving channels from a rigid but stretch-free ID to LMs more prone to strain. Also, of note, slow recovery from

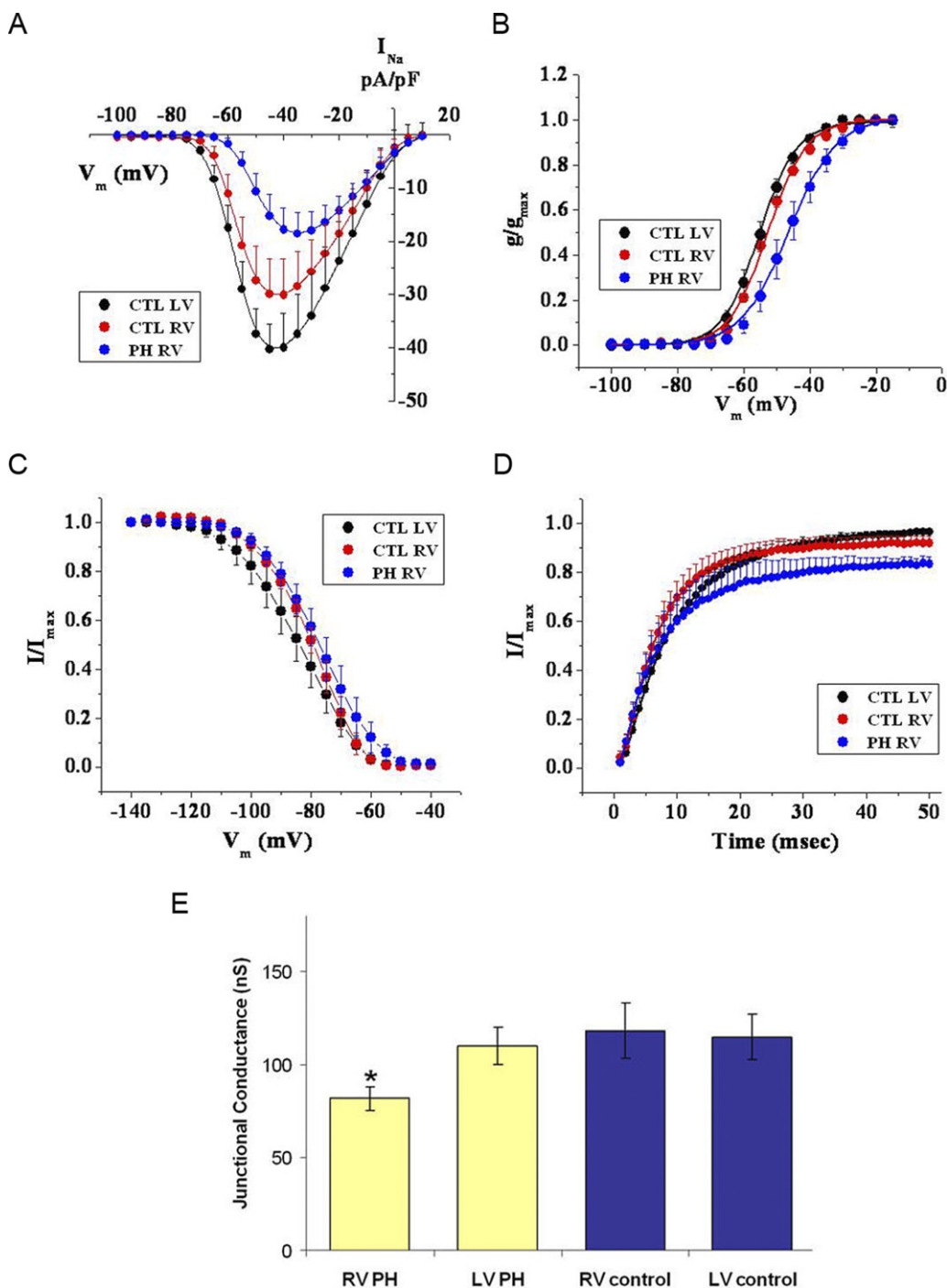


Figure 4 Electrophysiological changes. Electrophysiological analysis of ventricular myocytes dissociated from PH-afflicted sheep hearts. **A–D:** Peak average sodium current density (**A**), steady-state activation (**B**), steady-state inactivation (**C**), and recovery from inactivation kinetics (**D**) in ventricular myocytes dissociated from right ventricle (PH RV, blue) or left ventricle (CTL LV, black) of PH-afflicted sheep hearts, as well as from the RV of a control animal (CT LRV, red). **E:** Junctional conductance measured from cell pairs obtained from either the LV or the RV of control (blue) or PH-afflicted animals (yellow). PH = pulmonary hypertension.

inactivation was observed in our previous studies after silencing PKP2,¹ suggesting that composition of the macromolecular complex that includes Nav1.5 can determine its kinetic properties.

Cx43-containing connexons are delivered to the plasma membrane in vesicles moving along microtubules.^{12,13} EB1 serves as a guide for the microtubule

growth and vesicle delivery.²⁶ N-cadherin plays an essential role by tethering EB1 and, as a result, Cx43-containing vesicles to the membrane.²⁶ Immunohistochemical studies revealed that EB1 signal is enriched at the ID.³⁴ On the other hand, in the heart with ischemic cardiomyopathy, the decrease in Cx43 signal at the ID correlated with loss of EB1 enrichment.³⁴ Here, we find

Table 1 Parameters of I_{Na} recorded from sheep ventricular myocytes

	$I_{Na,peak}$ (pA)	$V_{1/2,activation}$ (mV)	$V_{1/2,inactivation}$ (mV)	Recovery time constants (ms)
CTL LV	-43.83 ± 7.67 (8)*	-55.47 ± 1.13 (8)†	-85.82 ± 3.76 (8)	9.69 ± 1.29 (8)
CTL RV	-30.17 ± 6.77 (4)	-53.05 ± 0.91 (4)‡	-79.67 ± 1.87 (3)	6.58 ± 0.81 (3)
PH RV	-18.64 ± 3.9 (7)	-44.09 ± 2.41 (7)	-76.47 ± 3.3 (7)	9.07 ± 3.23 (6)

The numbers in parentheses indicate the number of experiments.

CTL = control; I_{Na} = sodium current; LV = left ventricle; PH = pulmonary hypertension; RV = right ventricle.

* $P < .05$ for CTL LV vs PH RV.

† $P < .001$ for CTL LV vs CTL RV.

‡ $P < .05$ for CTL RV vs PH RV.

enrichment of immunoreactive EB1 with lateralized gap junctions. The presence of EB1 signal at the LM suggests that forward trafficking of Cx43 is not disrupted but rather preserved and redirected to a different location. This notion is further supported by the finding that Kif5b, an isoform of the motor protein Kinesin-1, also redistributed to LMs in PH hearts. While we do not have direct evidence that Cx43-containing vesicles are driven by kinesin-1 motors, the hypothesis is consistent with recent in vitro studies showing that Cx32 in vesicles isolated from hepatocytes is driven along microtubules by Kinesin-1.²⁹ Whether Cx43 lateralization depends on Kif5b remains a matter of future studies.

In summary, we have found that in a large animal model of RV pressure overload, loss of gap junctions at the ID was accompanied by reorganization of junctional complexes in a direction parallel to fiber orientation. We postulate that the latter involves (a) redirectionality of microtubule-mediated forward trafficking and (b) assembly of mechanical junctions that stabilize newly formed gap junction plaques. We speculate that this remodeling may be critical for the preservation of electrical synchrony in the afflicted tissue, despite changes in the localization and electrical properties of $Na_v1.5$. As such, lateralization may not always be an arrhythmogenic substrate but, at least in this instance, an adaptive mechanism that prevents uncoupling and arrhythmias in the heart.

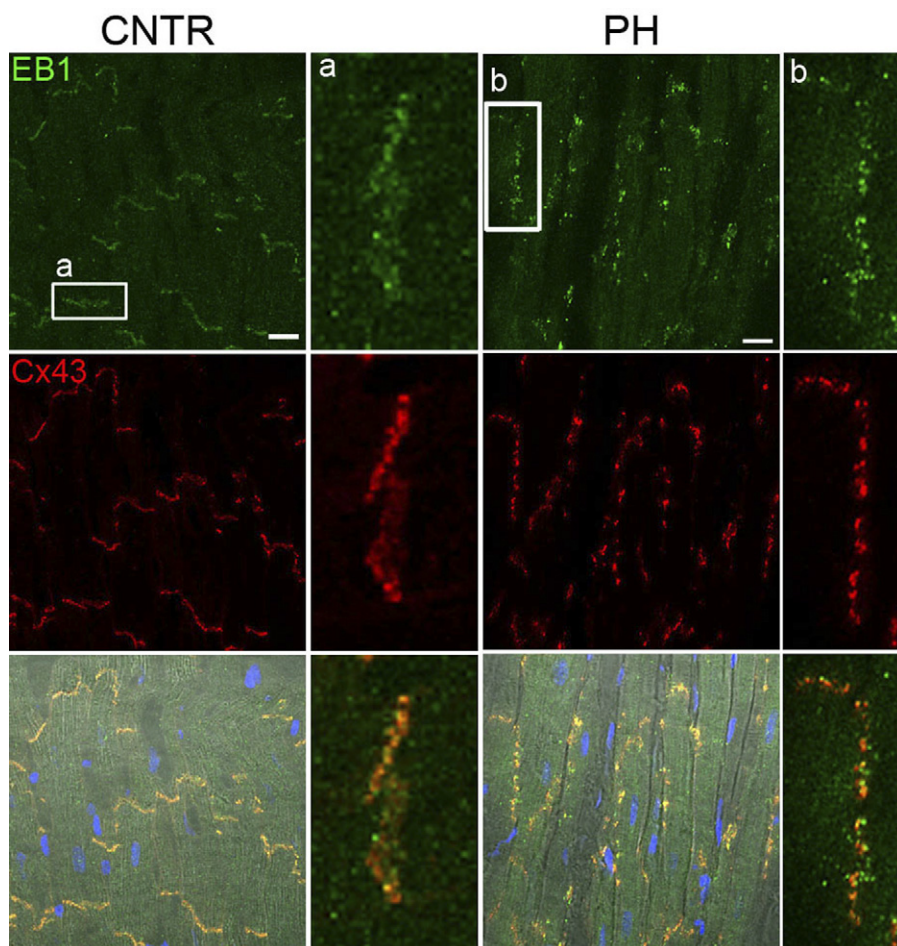


Figure 5 Localization of EB1. Confocal microscopy image obtained from right ventricular tissue of CNTR or PH sheep. EB1 (green), Cx43 (red), nuclei (TO-PRO-3, blue). **a** and **b**: Enlarged areas of intercalated disc in CNTR (**a**) and PH (**b**) tissue. Notice that the area is rotated 90° clockwise in (**a**). Scale bar = 20 μ m. CNTR = control; Cx43 = connexin43; PH = pulmonary hypertension.

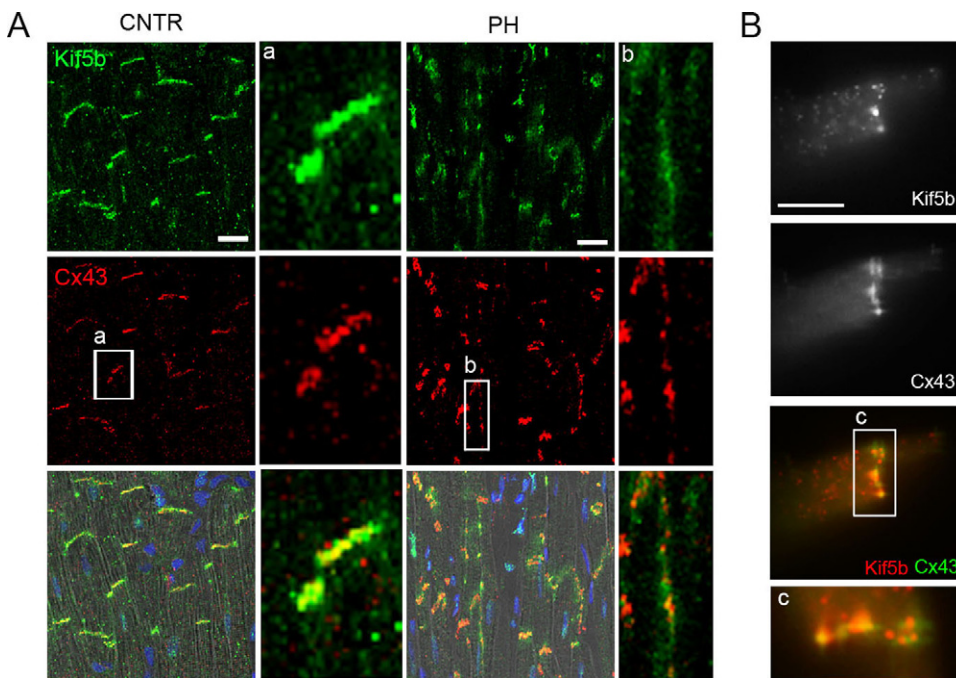


Figure 6 Redirection of Kinesin-1 to the lateral membrane. **A:** Confocal microscopy image obtained from right ventricular tissue of CNTR or PH sheep. Kif5b (green), Cx43 (red), nuclei (TO-PRO-3, blue). **a:** Enlarged image of Cx43 with Kif5b at the intercalated disc in CNTR. **b:** Enlarged image of Cx43 with Kif5b along the long axis. Scale bar = 20 μm . **B:** Localization of Kif5b. TIRF microscopy images obtained from freshly isolated mouse ventricular cardiomyocyte. Notice colocalization of immunoreactive Kif5b and Cx43 (merged panel at the bottom, from box labeled "c"). Scale bar = 5 μm . CNTR = control; Cx43 = connexin43; PH = pulmonary hypertension; TIRF = total internal reflection fluorescence.

References

- Sato PY, Coombs W, Lin X, et al. Loss of plakophilin-2 expression leads to decreased sodium current and slower conduction velocity in cultured cardiac myocytes. *Circ Res* 2009;105:523–526.
- Sato PY, Coombs W, Lin X, et al. Interactions between ankyrin-G, plakophilin-2, and connexin43 at the cardiac intercalated disc. *Circ Res* 2011;109:193–201.
- Delmar M, Liang FX. Connexin43, and the regulation of intercalated disc function. *Heart Rhythm* November 2, 2011. Epub ahead of print.
- Tan XY, He JG. The remodeling of connexin in the hypertrophied right ventricular in pulmonary arterial hypertension and the effect of a dual ET receptor antagonist (bosentan). *Pathol Res Pract* 2009;205:473–482.
- Qu J, Volpicelli FM, Garcia LI, et al. Gap junction remodeling and spironolactone-dependent reverse remodeling in the hypertrophied heart. *Circ Res* 2009;104:365–371.
- Akar FG, Nass RD, Hahn S, et al. Dynamic changes in conduction velocity and gap junction properties during development of pacing-induced heart failure. *Am J Physiol Heart Circ Physiol* 2007;293:H1223–H1230.
- Cabo C, Yao J, Boyden PA, et al. Heterogeneous gap junction remodeling in reentrant circuits in the epicardial border zone of the healing canine infarct. *Cardiovasc Res* 2006;72:241–249.
- Barker RJ, Price RL, Gourdie RG. Increased association of ZO-1 with connexin43 during remodeling of cardiac gap junctions. *Circ Res* 2002;90:317–324.
- Uzzaman M, Honjo H, Takagishi Y, et al. Remodeling of gap junctional coupling in hypertrophied right ventricles of rats with monocrotaline-induced pulmonary hypertension. *Circ Res* 2000;86:871–878.
- Peters NS, Coromilas J, Severs NJ, Wit AL. Disturbed connexin43 gap junction distribution correlates with the location of reentrant circuits in the epicardial border zone of healing canine infarcts that cause ventricular tachycardia. *Circulation* 1997;95:988–996.
- Rohr S. Molecular crosstalk between mechanical and electrical junctions at the intercalated disc. *Circ Res* 2007;101:637–639.
- Lauf U, Giepmans BN, Lopez P, Braconnot S, Chen SC, Falk MM. Dynamic trafficking and delivery of connexons to the plasma membrane and accretion to gap junctions in living cells. *Proc Natl Acad Sci U S A* 2002;99:10446–10451.
- Thomas T, Jordan K, Simek J, et al. Mechanisms of Cx43 and Cx26 transport to the plasma membrane and gap junction regeneration. *J Cell Sci* 2005;118:4451–4462.
- Kucera JP, Rohr S, Rudy Y. Localization of sodium channels in intercalated disks modulates cardiac conduction. *Circ Res* 2002;91:1176–1182.
- Dominguez JN, de la Rosa A, Navarro F, Franco D, Aranea AE. Tissue distribution and subcellular localization of the cardiac sodium channel during mouse heart development. *Cardiovasc Res* 2008;78:45–52.
- Maier SK, Westenbroek RE, McCormick KA, Curtis R, Scheuer T, Catterall WA. Distinct subcellular localization of different sodium channel alpha and beta subunits in single ventricular myocytes from mouse heart. *Circulation* 2004;109:1421–1427.
- Thabut G, Dauriat G, Stern JB, et al. Pulmonary hemodynamics in advanced COPD candidates for lung volume reduction surgery or lung transplantation. *Chest* 2005; 127:1531–1536.
- Thabut G, Mal H, Castier Y, et al. Survival benefit of lung transplantation for patients with idiopathic pulmonary fibrosis. *J Thorac Cardiovasc Surg* 2003;126:469–475.
- Weitzenblum E, Ehrhart M, Rasaholjanahary J, Hirth C. Pulmonary hemodynamics in idiopathic pulmonary fibrosis and other interstitial pulmonary diseases. *Respiration* 1983;44:118–127.
- Vizza CD, Lynch JP, Ochoa LL, Richardson G, Trulock EP. Right and left ventricular dysfunction in patients with severe pulmonary disease. *Chest* 1998;113:576–583.
- Sato H, Hall CM, Griffith GW, et al. Large animal model of chronic pulmonary hypertension. *ASAIO J* 2008;54:396–400.
- Pohlmann JR, Akay B, Camboni D, Koch KL, Mervak BM, Cook KE. A low mortality model of chronic pulmonary hypertension in sheep. *J Surg Res*. In press.
- Lettieri CJ, Nathan SD, Barnett SD, Ahmad S, Shorr AF. Prevalence and outcomes of pulmonary arterial hypertension in advanced idiopathic pulmonary fibrosis. *Chest* 2006;129:746–752.
- Della Rocca G, Pugliese F, Antonini M, et al. Hemodynamics during inhaled nitric oxide in lung transplant candidates. *Transplant Proc* 1997;29:3367–3370.
- Venuta F, Rendina EA, Rocca GD, et al. Pulmonary hemodynamics contribute to indicate priority for lung transplantation in patients with cystic fibrosis. *J Thorac Cardiovasc Surg* 2000;119:682–689.
- Shaw RM, Fay AJ, Puthenveedu MA, von Zastrow M, Jan YN, Jan LY. Microtubule plus-end-tracking proteins target gap junctions directly from the cell interior to adherens junctions. *Cell* 2007;128:547–560.
- Zadeh AD, Cheng Y, Xu H, et al. Kif5b is an essential forward trafficking motor for the Kv1.5 cardiac potassium channel. *J Physiol* 2009;587:4565–4574.
- Argyropoulos G, Stutz AM, Ilnytska O, et al. *KIF5B* gene sequence variation and response of cardiac stroke volume to regular exercise. *Physiol Genomics* 2009;36: 79–88.
- Fort AG, Murray JW, Dandachi N, et al. In vitro motility of liver connexin vesicles along microtubules utilizes kinesin motors. *J Biol Chem* 2011;286:22875–22885.
- Maass K, Shibayama J, Chase SE, Willecke K, Delmar M. C-terminal truncation of connexin43 changes number, size, and localization of cardiac gap junction plaques. *Circ Res* 2007;101:1283–1291.
- Borrmann CM, Grund C, Kuhn C, Hofmann I, Pieperhoff S, Franke WW. The area composita of adhering junctions connecting heart muscle cells of vertebrates. II: colocalizations of desmosomal and fascia adherens molecules in the intercalated disk. *Eur J Cell Biol* 2006;85:469–485.
- Franke WW, Borrmann CM, Grund C, Pieperhoff S. The area composita of adhering junctions connecting heart muscle cells of vertebrates. I: molecular definition in intercalated disks of cardiomyocytes by immunoelectron microscopy of desmosomal proteins. *Eur J Cell Biol* 2006;85:69–82.
- Beyder A, Rae JL, Bernard C, Stregge PR, Sachs F, Farrugia G. Mechanosensitivity of Nav1.5, a voltage-sensitive sodium channel. *J Physiol* 2010;588:4969–4985.
- Smyth JW, Hong TT, Gao D, et al. Limited forward trafficking of connexin43 reduces cell-cell coupling in stressed human and mouse myocardium. *J Clin Invest* 2010;120:266–279.

Methods

Sheep pulmonary hypertension model

A large animal model was created to simulate chronic pulmonary hypertension with right ventricular hypertrophy. This model effectively reproduces pulmonary hemodynamics experienced by lung transplant candidates with pulmonary hypertension secondary to respiratory dysfunction,^{1–7} and is described in more detail elsewhere.^{8,9} Sephadex beads (0.375 g) were suspended in sterile saline and injected into the pulmonary circulation of adult sheep every day for 60 days. Prior to heart harvest, sheep were anesthetized, a left thoracotomy was performed, and hearts instrumented according to published methods to measure mean pulmonary artery pressure, mean left atrial pressure and cardiac output. Details on the model, and hemodynamic parameters of the animal population used for these studies, have been published elsewhere.⁸

Immunofluorescence analysis

For cryosections, fragments of sheep hearts were flash frozen in Tissue Tec O.C.T. (Optimal Cutting Temperature Compound, Sakura, Sakura Finetek U.S.A., Inc., Torrance, CA) and stored at -80°C until they were sectioned. Sections were rehydrated by incubation in PBS and then fixed in 4% paraformaldehyde in PBS. Sections were then immersed in blocking buffer (2% Normal Goat Serum (NGS) 0.1% Triton-X100 in PBS) for 30 min at room temperature, followed by a one-hour incubation in primary antibodies. Sections were washed with PBS and incubated for 30 minutes with secondary antibodies (both primary and secondary antibodies were diluted in blocking buffer). Sections were washed and during the last wash they were incubated for 10 min in TO-PRO-3 (1 μM) in PBS. Samples were mounted using ProLong Gold (Invitrogen). Immunostained preparations were analyzed by confocal microscopy to determine protein localization in relation to cell morphology. TIRF (total internal reflection fluorescence) microscopy was used to conduct high spatial resolution imaging of Kif5b and Cx43 molecules at the cell membrane.

Primary antibodies were: for Cx43, #AB1728; rabbit; epitope: carboxyl-terminal domain, Chemicon International Inc, Temecula, CA; for Cx43, #C8093; mouse; Sigma-Aldrich, St. Louis, MO; for Cx43NT1, clone P1E11, mouse; epitope: N-terminus; Fred Hutchinson Cancer Research Center, Seattle, WA; plakophilin 2, #K44262M, Biodesign International, Saco, ME; for desmoplakin1/2, #2722–5204, AbD Serotec, Oxford, UK; Plakoglobin #610254, BD Transduction Laboratories, for desmoglein 1& 2, # 10R-D105A, Fitzgerald, Acton, MA; for Ankyrin G #33–8800, mouse, Invitrogen, Camarillo, CA; for N-cadherin, #610921, mouse, BD Transduction Laboratories; for Kinesin, # ab5629, rabbit, abcam, Cambridge, MA; for EB1, #610534, mouse, BD Transduction Laboratories; for Nav1.5 #ab56240, rabbit, abcam, Cambridge, MA. Secondary antibodies included goat anti-mouse and anti-rabbit IgG antibodies conjugated to Alexa Fluor 594 (Molecular

Probes, Eugene, OR), goat anti-mouse and anti-rabbit IgG antibodies conjugated to Alexa Fluor 488 (Molecular Probes), goat anti-mouse IgG antibodies conjugated to Alexa Fluor 647 and goat anti-rabbit IgG antibodies conjugated to Alexa Fluor 555. Immunofluorescence analyses were carried out on 5 μm cryosections of sheep ventricular tissue.

A “plaque” was defined as a cluster of 15 or more contiguous pixels showing an identifiable immunoreactive signal (smaller clusters were not measured). Most plaques were best defined as ellipsoids, with a long axis oriented either parallel (0 to 45 degrees) or perpendicular (46 to 90 degrees) to the orientation of the fibers (defined by the long axis of the nuclei of the cells surrounding the plaque). In cases where plaques did not have a well-defined long axes (plaques that were circular or irregularly shaped), the plaque orientation was considered as “ambiguous.” Numbers of plaques of a given direction were counted to establish the prevalence of lateralization of a particular protein in PH sheep versus control. The extent of co-localization of Cx43 with another protein (regardless of orientation) was defined by a Pearson’s Colocalization Coefficient, estimated using MacBiophotonics ImageJ and WCIF ImageJ (NIH).

Western blot

Collected tissue was frozen and stored at -80°C . Prior to use, tissue was thawed and homogenized in a lysate buffer that contained protease inhibitors (Roche). Protein Assay was performed. Samples were heated for 10 min at 55°C and 25 μg of each sample was loaded in a 4–12% 15-well Tris-Glycine gel, and run at 120V. Samples were transferred to a nitrocellulose membrane at 110V for 90min. Blocking of the nonspecific signal was done by incubating membranes in “blocking buffer” (5%NFM in T-PBS). Incubation with primary antibodies was done overnight at 4°C in blocking buffer. Incubation with secondary antibodies was done for an hour at room temperature in PBS. Protein detection was performed using Odyssey infrared imaging system (LI-COR).

Primary antibodies used: for Cx43 #C6219, rabbit, Sigma-Aldrich, St.Louis, MO; for Ankyrin G, # sc-28561, rabbit, Santa Cruz Biotechnology, N-cadherin, # 610921, mouse, BD Transduction Laboratories; Plakoglobin #610254, BD Transduction Laboratories; for α -tubulin, # T5168, mouse, Sigma-Aldrich or # ab18251, rabbit, abcam; for α -tubulin, ab18251, rabbit, abcam, Cambridge, MA. Secondary antibodies: IRDye 800CW Donkey anti-rabbit IgG, # 926–32213, LI-COR, Lincoln, Nebraska and IRDye 680 Conjugated Goat anti-mouse IgG, # 926–32220, LI-COR.

Transmission electron microscopy (TEM)

For TEM analysis, the free wall of the right ventricle was excised and sectioned into small pieces. The pieces were fixed overnight at 4°C in 2.5% glutaraldehyde and 2.0% paraformaldehyde and post fixed in 1% osmium tetroxide. After washing, they were stained with saturated uranyl ac-

etate, and embedded in Epon 812. Ultra-thin sections were prepared and stained with saturated uranyl acetate and lead citrate. The sections were examined with a Philips CM100 transmission electron microscope, at an accelerating voltage of 60 kV. The sections were examined at low magnification (2,600x) and were re-photographed at a final print magnification of 34,000x.

Total internal reflection fluorescence (TIRF)

TIRF was conducted on immunolabeled isolated mouse myocytes. Immediately following dissociation, cells were plated on laminin coated glass bottom dishes (MatTek), fixed (4% paraformaldehyde) and immunolabeled as described above.

Electrophysiology

Whole-cell cardiac sodium current (I_{Na}) was recorded from freshly isolated sheep myocytes using standard methods. All recordings were conducted at room temperature, in a low-sodium extracellular solution containing (in mM): NaCl, 5; MgCl₂, 1; CaCl₂, 1.8; CdCl₂, 0.1; HEPES, 20; CsCl, 132.5; glucose, 11. The pipette solution contained (in mM): NaCl, 5; CsF, 135; EGTA, 10; MgATP, 5; HEPES, 5. Recordings were performed using an Axopatch-200B Amplifier (Molecular Devices Sunnyvale, CA) and data acquisition and analysis were performed utilizing pClamp10.2 software (Molecular Devices Sunnyvale, CA). Pipette resistances ranged from 2–3 M Ω . Access resistance was compensated to 1–2 M Ω . Input resistance was 500 M Ω to 1 G Ω . To characterize the voltage dependence of the peak I_{Na} , single cells were held at -160 mV, and 200 msec voltage steps were applied from -100 to $+10$ mV in 5 mV increments. Interval between voltage steps was 3 sec. Voltage-dependence of inactivation was assessed by holding cells at various potentials from -140 to -40 mV followed by a 30 msec test pulse to -40 mV to elicit I_{Na} . Recovery from inactivation was studied by holding cells at -160 mV and applying two 20-msec test pulses (S1, S2) to -45 mV separated by variable inter-pulse intervals, to a maximum S1–S2 interval of 80 msec. The S1–S1 interval was kept constant at 3 sec.

The dual whole-cell voltage clamp technique was used to record gap junction currents. G_j was measured from cells in side to side apposition. Both cells in the pair (cell1 and cell2) were independently voltage clamped at the same

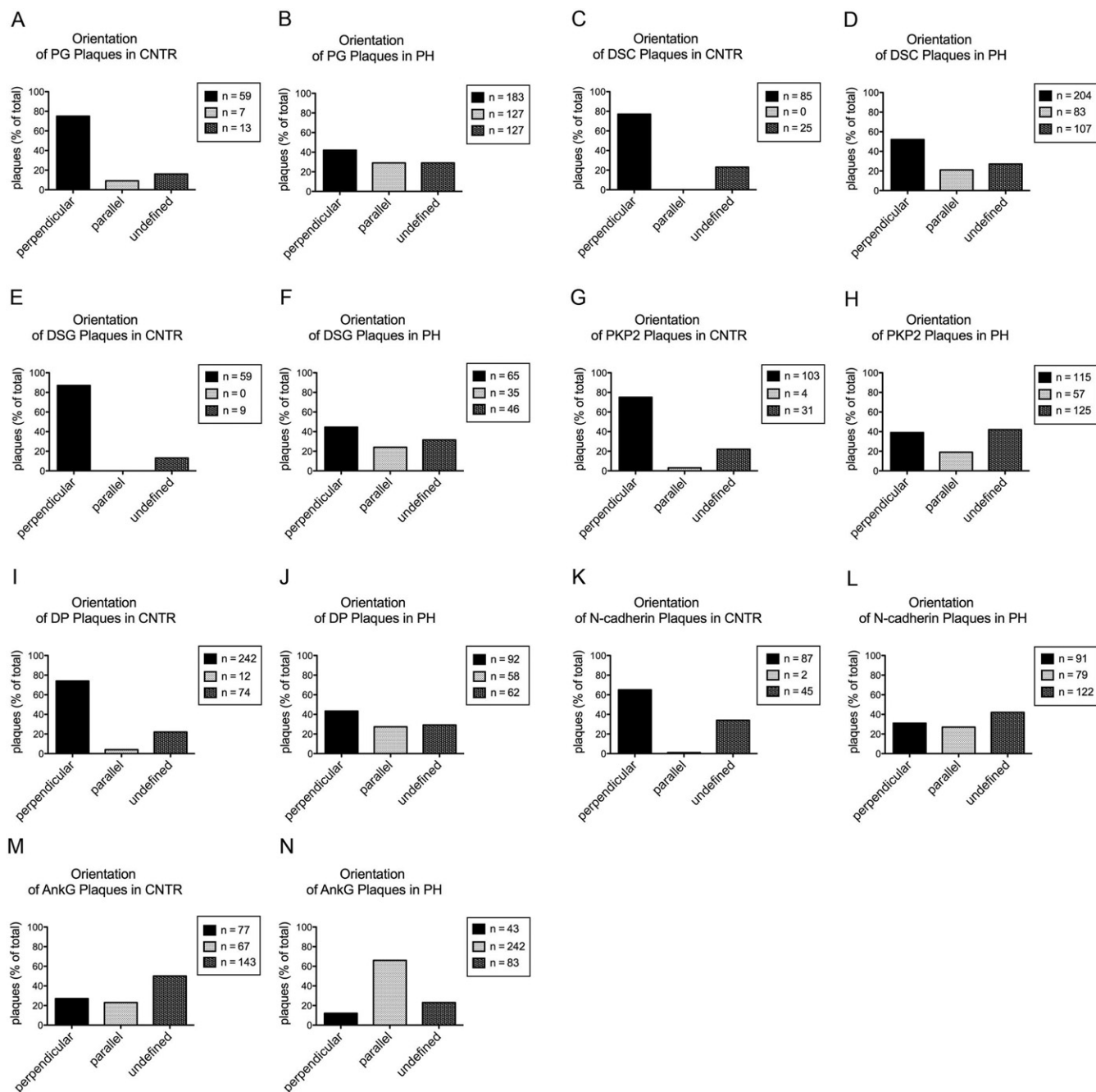
holding potential (-40 mV). The prejunctional cell (cell1) was stepped to $+20$ mV, creating a potential difference across the junction (V_j) of $+60$ mV during repetitive 10–30-s steps. Patch pipettes were filled with a solution containing cesium (in mM: 130 CsCl; 0.5 CaCl₂; 10 HEPES; 10 EGTA; 2.0 Na₂ATP; 3.0 MgATP; pH 7.2). Pipette resistance was 3.0–5.0 M Ω . During recording, cells were kept at room temperature in a cesium-containing solution (in mM: 160 NaCl; 10 CsCl; 2.0 CaCl₂; 0.6 MgCl₂; 10 HEPES; pH 7.4).

Statistical analysis

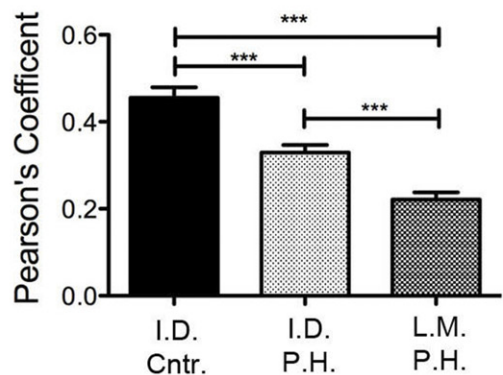
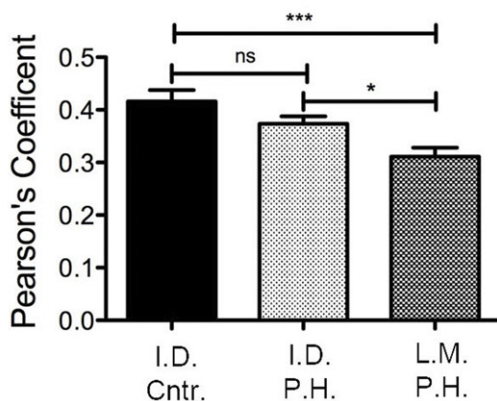
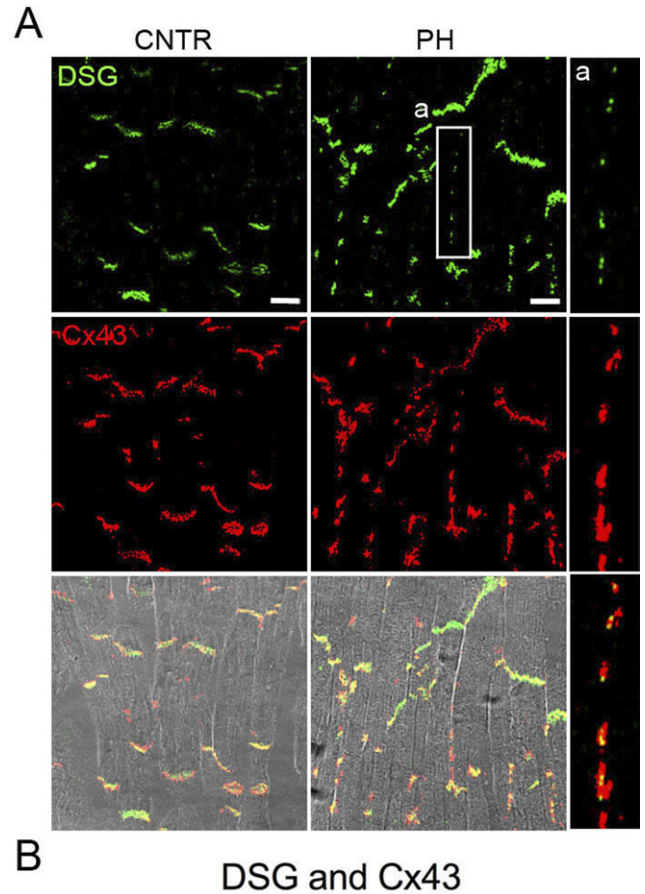
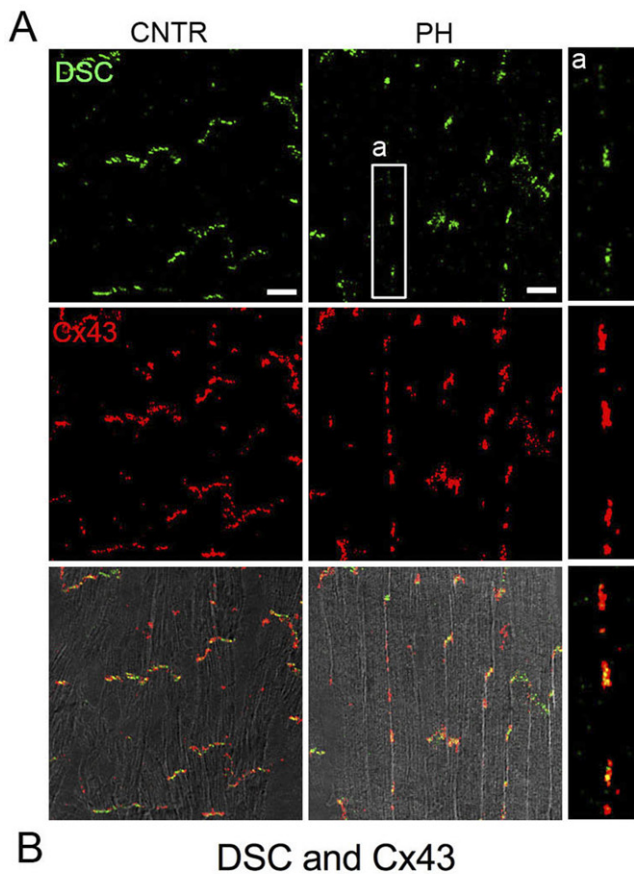
Statistical significance for measurements of sodium and gap junction current properties was assessed by unpaired two-tailed *t* test (Origin Version 7.0; Origin Laboratory Corporation). For immunochemical data, statistical significance was assessed by unpaired 2-tailed *t* test, and, for multiple groups, Tukey's Multiple Comparison One-way ANOVA, (GraphPad Prism). All data are presented as mean value \pm S.E.M. Statistical significance was set at $P < 0.05$.

References

1. Lettieri CJ, Nathan SD, Barnett SD, Ahmad S, Shorr AF. Prevalence and outcomes of pulmonary arterial hypertension in advanced idiopathic pulmonary fibrosis. *Chest* 2006;129:746–752.
2. Vizza CD, Lynch JP, Ochoa LL, Richardson G, Trulock EP. Right and left ventricular dysfunction in patients with severe pulmonary disease. *Chest* 1998;113:576–583.
3. Weitzenblum E, Ehrhart M, Rasaholinjanahary J, Hirth C. Pulmonary hemodynamics in idiopathic pulmonary fibrosis and other interstitial pulmonary diseases. *Respiration* 1983;44:118–127.
4. Thabut G, Mal H, Castier Y, et al. Survival benefit of lung transplantation for patients with idiopathic pulmonary fibrosis. *J Thorac Cardiovasc Surg* 2003;126:469–475.
5. Thabut G, Dauriat G, Stern JB, et al. Pulmonary hemodynamics in advanced COPD candidates for lung volume reduction surgery or lung transplantation. *Chest* 2005;127:1531–1536.
6. Della Rocca G, Pugliese F, Antonini M, et al. Hemodynamics during inhaled nitric oxide in lung transplant candidates. *Transplant Proc* 1997;29:3367–3370.
7. Venuta F, Rendina EA, Rocca GD, et al. Pulmonary hemodynamics contribute to indicate priority for lung transplantation in patients with cystic fibrosis. *J Thorac Cardiovasc Surg* 2000;119:682–689.
8. Sato H, Hall CM, Griffith GW, et al. Large animal model of chronic pulmonary hypertension. *ASAIO J* 2008;54:396–400.
9. Pohlmann JR AB, Camboni D, Koch KL, Mervak BM, Cook KE. A low mortality model of chronic pulmonary hypertension in sheep. *Surgical Research*, in press. *Surgical Research*.

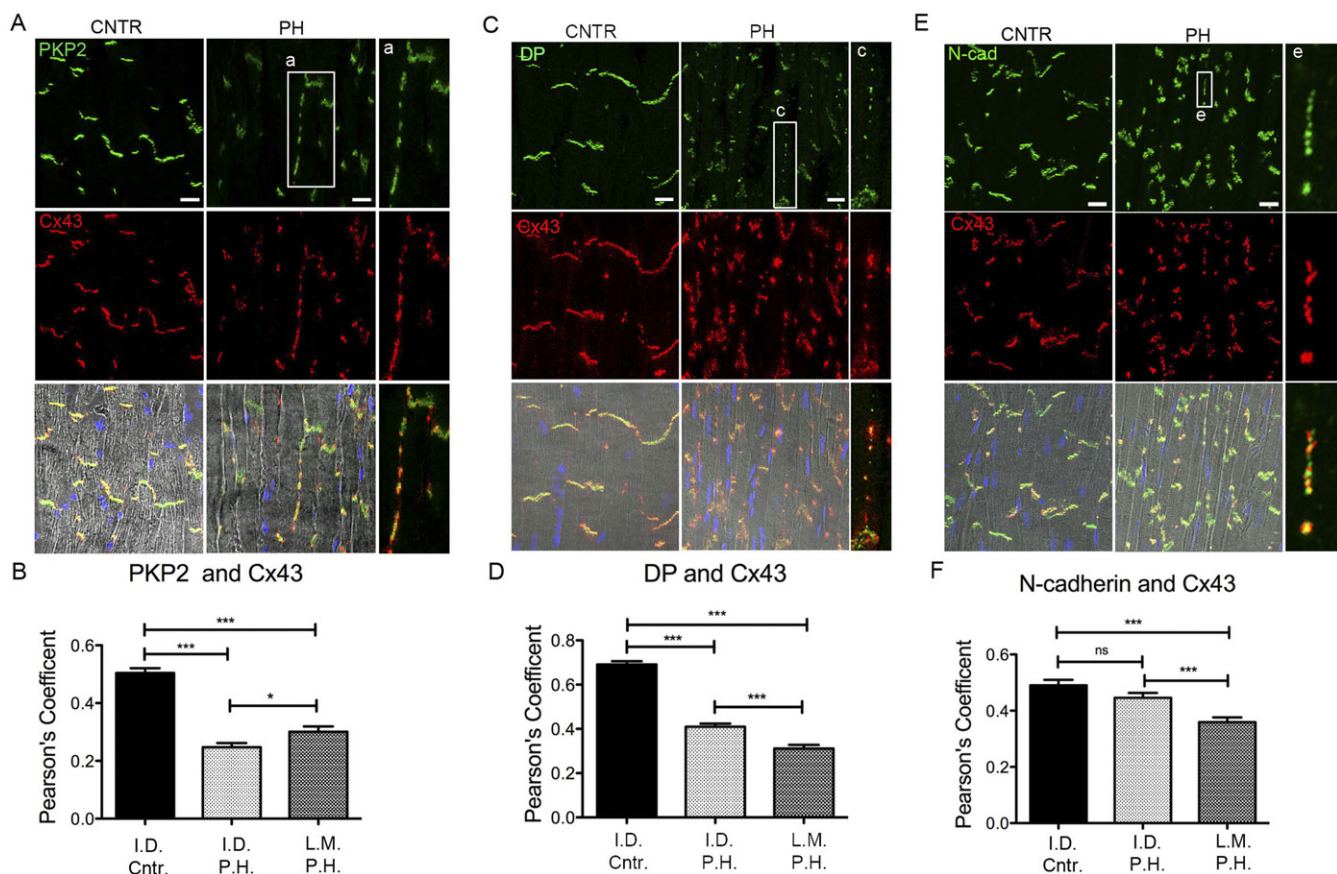


Supplemental Figure 1 Plaque orientation. Quantification plots representing percentage of PG (A, B), DSC (C, D), DSG (E, F), PKP2 (G, H), DP (I, J), N-cadherin (K, L), and AnkG (M, N) plaques found in different fields of confocal microscopy images in CNTR (A, C, E, G, I, K, and M) or PH (B, D, F, H, J, L, and M). Total number of plaques analyzed: 79, 437 (A, B), 110, 394 (C, D), 68, 146 (E, F), 138, 297 (G, H), 328, 212 (I, J), 134, 292 (K, L), and 287, 368 (M, N).

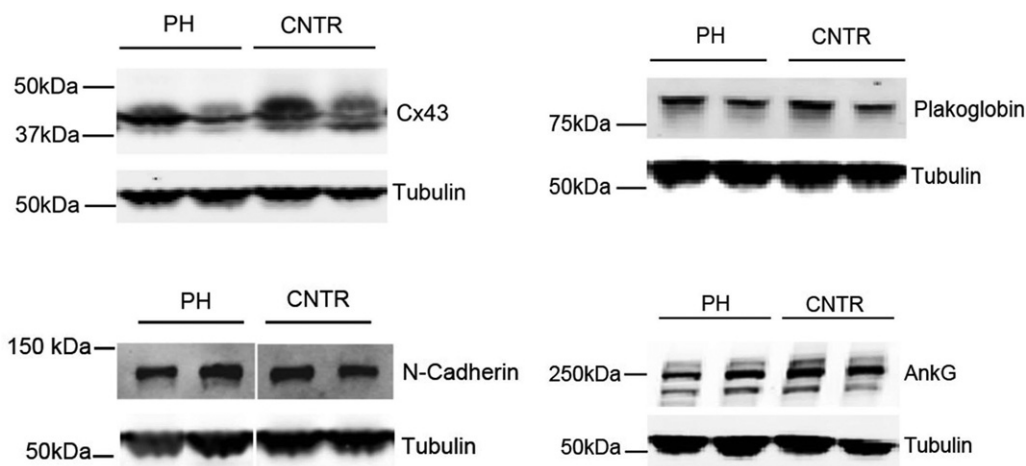


Supplemental Figure 2 Localization of Desmocollin. **A**, Confocal microscopy image obtained from right ventricular tissue of control sheep (CNTR) or sheep afflicted with pulmonary hypertension (PH). Desmocollin (DSC; green), Cx43 (red). Bar, 20 μ m. **B**, Colocalization (Pearson's Coefficient) of DSC and Cx43 signals in plaques oriented perpendicular (intercalated disc; I.D.) or parallel (lateral membrane; L.M.) to the fiber orientation. Statistical analysis: One-way ANOVA, Tukey's Multiple Comparison Test. Mean \pm SEM. p values: >0.05 (ns); 0.01 to 0.05 (*); 0.001 to 0.0001 (***). Numbers of regions of interest analyzed: 40, 60, and 60 for I.D. Cntr., I.D. P.H., and L.M. P.H., respectively.

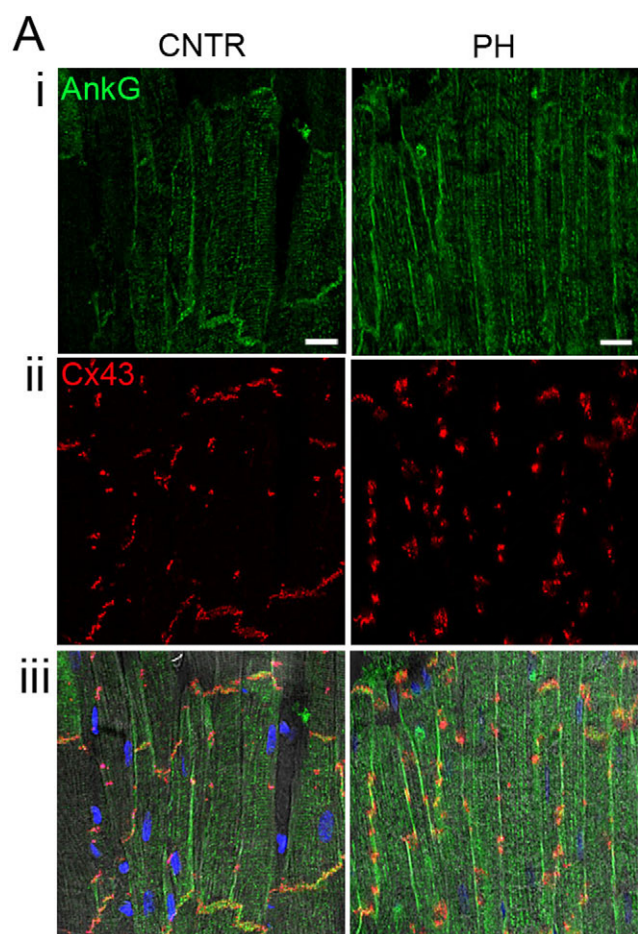
Supplemental Figure 3 Localization of Desmoglein. **A**, Confocal microscopy image obtained from right ventricular tissue of control sheep (CNTR) or sheep afflicted with pulmonary hypertension (PH). Desmoglein, DSG; green. Connexin43, Cx43, red. Nuclei, TO-PRO-3, blue. **a**, enlarged images of Cx43 with DSG along the long axis. Bar, 20 μ m. **B**, Colocalization (Pearson's Coefficient) of DSG and Cx43 in plaques oriented perpendicular (intercalated disc; I.D.) or parallel (lateral membrane; L.M.) to the fiber orientation. Statistical analysis: ANOVA, Tukey's Multiple Comparison Test. Mean \pm SEM. p value < 0.001 (***). Numbers of regions of interest analyzed: 32, 54, and 54 for I.D. Cntr., I.D. P.H., and L.M. P.H., respectively.



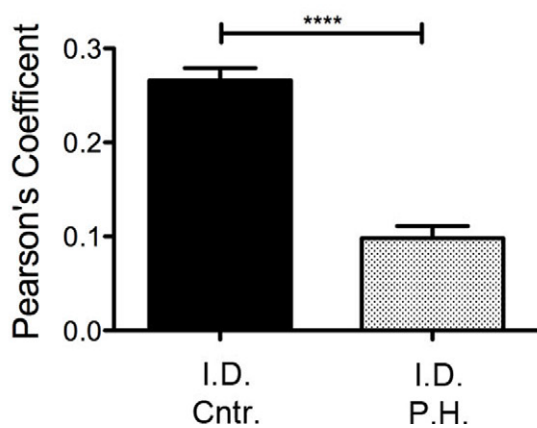
Supplemental Figure 4 Localization of PKP2, DP and N-cadherin. A, C, E Confocal microscopy images obtained from the right ventricles of control sheep (CNTR) or sheep afflicted with pulmonary hypertension (PH). PKP2: Plakophilin-2; DP: Desmoplakin; N-Cad: N-Cadherin; Cx43:Connexin43. nuclei labeled with TO-PRO-3 (blue). a, c, e, enlarged images of Cx43 and PKP2, DP, or N-cad along the long axis. Bar, 20 μ m. B, Quantification of colocalization (Pearson's Coefficient) of PKP2 and Cx43 signals at the areas of intercalated disc (I.D.) in CNTR and PH animals, and at the lateral membrane (L.M.) of PH animals. Statistical analysis: ANOVA, Tukey's Multiple Comparison Test. Mean \pm SEM. p values: p >0.05 (ns); p 0.01 to 0.05 (*); p value 0.001 to 0.01 (**); p value 0.001 to 0.0001 (***). Numbers of regions of interest analyzed (N): 44, 115, and 67 for I.D. Cntr., I.D. P.H., and L.M. P.H., respectively. D, Quantification of Colocalization (Pearson's Coefficient) of DP and Cx43. N = 48, 69, and 67 for I.D. Cntr., I.D. P.H., and L.M. P.H., respectively. E, Quantification of colocalization of N-cadherin and Cx43 signals. N = 39, 57, and 51 for I.D. Cntr., I.D. P.H., and L.M. P.H., respectively.



Supplemental Figure 5 Western Blot analysis of CNTR and PH hearts. Duplicate examples of western blots for Cx43, N-cadherin, plakoglobin and AnkG showing no changes in protein abundance when compared signal from PH hearts to control (CNTR).



B AnkG and Cx43



Supplemental Figure 6 Ankyrin-G and Cx43. **A:** Confocal microscopy images obtained from right ventricular tissue of control sheep (CNTR) or sheep afflicted with pulmonary hypertension (PH). Immunoreactive Ankyrin-G (AnkG; green) and Cx43 (red) are presented separately (I, ii) or in a merged image (iii). Nuclei (TO-PRO-3) in blue. **B:** Pearson's coefficient showing the difference in co-localization of AnkG and Cx43 in control, when compared to the PH hearts. Statistical analysis: Unpaired t test. Mean \pm SEM. $p < 0.0001$ (****) Scale bar: 20 μ m.